

Dynamics of *n*-Hexane Inside Silicalite, As Studied by  $^2\text{H}$  NMRAlexander G. Stepanov,<sup>\*,†,‡</sup> Alexander A. Shubin,<sup>†</sup> Mikhail V. Luzgin,<sup>†</sup> Timur O. Shegai,<sup>‡</sup> and Hervé Jobic<sup>\*,§</sup>

Boriskov Institute of Catalysis, Siberian Branch of the Russian Academy of Sciences, Prospekt Akademika Lavrentieva 5, Novosibirsk 630090, Russia, Department of Natural Sciences, Novosibirsk State University, Pirogova Street 2, Novosibirsk 630090, Russia, and Institut de Recherches sur la Catalyse, CNRS, 2 av. Albert Einstein, 69626 Villeurbanne, France

Received: January 14, 2003; In Final Form: April 22, 2003

Perdeuterated *n*-hexane, adsorbed in silicalite, has been found to exhibit a  $^2\text{H}$  NMR spectrum that represents a superposition of three Pake-powder patterns. Two Pake-powder patterns, with the spectral parameters  $C_Q = 23.5$  kHz and  $\eta = 0$  and  $C_Q = 30.1$  kHz and  $\eta = 0$  ( $C_Q$  represents quadrupole constants and  $\eta$  is the asymmetry parameter), belong to different methylene groups and one powder pattern, with  $C_Q = 7.0$  kHz and  $\eta = 0.7$ , arises from the methyl groups. The observed line shapes have been concluded to arise from the fast anisotropic translational and rotational motions of the alkane in the silicalite channels. The reduction of the quadrupole constants, in comparison to that in rigid *n*-hexane, and the appearance of an asymmetry parameter for the methyl groups have been interpreted in terms of three modes of motion exhibited by *n*-hexane inside the channel system: (a) rotation of the molecule about the channel axis; (b) trans/gauche conformational isomerization around nonterminal C–C bonds and rotation of the methyl groups around terminal C–C bonds; and (c) fast interchange of the adsorbed molecules between both straight and zigzag channels and along zigzag channels with an effective angle of  $\sim 90^\circ$  between adjacent sites of the molecule location during successive jumps. The proportion percentage of trans/gauche conformations is estimated to be 78/22, which exceeds that in gas phase or liquids. This demonstrates that constraining effects of the narrow silicalite pore walls retain the molecules in a more elongated conformation, compared to that in a gas phase or liquid. The rotation of a methyl group around a terminal C–C bond has been estimated to occur with a characteristic time of  $\sim 40$  ps at 300 K and an activation energy of 9.4 kJ/mol. The reorientation of methylene groups, corresponding either to conformational isomerization or to translational diffusion, occurs 1 order of magnitude slower, with a characteristic time of  $\sim 300$  ps and an activation energy of 7.5 kJ/mol.

## Introduction

ZSM-5 zeolite is widely used for the separation of hydrocarbons<sup>1,2</sup> and in catalysis.<sup>3</sup> The unique three-dimensional system of pores in ZSM-5,<sup>4,5</sup> comprising intersecting straight and zigzag channels ca. 5.5 Å in diameter and pore intersection voids  $\sim 9$  Å in diameter, provides a high efficiency for the separation of linear and branched hydrocarbons and represents the basis for the shape selectivity properties of this zeolite in catalytic performance. Detailed study of the dynamics of adsorbed hydrocarbon molecules with dimensions commensurate to the sizes of the zeolitic pores is of particular importance, because the molecular motion of the adsorbed hydrocarbon may have a close relation to the process of hydrocarbon separation<sup>6</sup> and to the shape selectivity exhibited by this zeolite.<sup>7</sup> Therefore, much experimental and theoretical work has been done to clarify the dynamic behavior of alkanes occluded in the pores of the zeolite ZSM-5 or silicalite,<sup>5</sup> which is the aluminum-free analogue of ZSM-5 (the correct nomenclature is silicalite-1, but we will use the term silicalite for simplicity). Pulsed-field-gradient (PFG) NMR<sup>8</sup> and quasi-elastic neutron scattering (QENS)<sup>9–13</sup> have access to the diffusivities of the adsorbed

molecules. Theoretical molecular dynamics (MD) simulations<sup>14–23</sup> provide us with information on the mechanism of diffusion; however, this information is limited, because the united atom representation is generally used, which means that only the backbone is considered, not the hydrogen atoms. This simplifies the simulations, but the rotation about the main molecular axis is not well represented and the methyl torsions are missing.

Deuterium solid-state NMR ( $^2\text{H}$  NMR) spectroscopy has been shown many times to be a powerful technique to probe the dynamics of alkanes,<sup>11,24,25</sup> alkenes,<sup>26</sup> alcohols,<sup>27–30</sup> and aromatics<sup>24,25,31</sup> in zeolitic pores.  $^2\text{H}$  NMR provides information on the peculiarities of the dynamics of both the separate groups and the molecule as a whole for the adsorbed alkane—that is, data that are complementary to PFG, QENS, and MD simulations. The line shape for  $^2\text{H}$  NMR, being defined completely by intramolecular quadrupole interaction,<sup>32–34</sup> is especially sensitive to the nature of molecular motion and its rate.<sup>32,33</sup> Spin–lattice relaxation time ( $T_1$ ) also brings information on the energetics and the rate of the different intramolecular and intermolecular motions.

In the present paper, we report the results of  $^2\text{H}$  NMR studies on the dynamic behavior of linear *n*-hexane inside silicalite. Interpretation of the separate line shapes contributing to the total  $^2\text{H}$  NMR spectrum of the adsorbed alkane and the temperature dependence of the spin–lattice relaxation time  $T_1$  is made in

\* Authors to whom correspondence should be addressed. E-mail: a.g.stepanov@catalysis.nsk.su, Herve.Jobic@catalyse.univ-lyon1.fr.

<sup>†</sup> Boriskov Institute of Catalysis.

<sup>‡</sup> Novosibirsk State University.

<sup>§</sup> Institut de Recherches sur la Catalyse, CNRS.

terms of different mobilities, exhibited by different CD<sub>n</sub> groups ( $n = 2, 3$ ) of the adsorbed alkane.

## Experimental Section

**Materials.** For the <sup>2</sup>H NMR experiments, the silicalite sample was prepared as described by Tuel and Ben Taarit.<sup>35</sup> The synthesized silicalite sample was characterized by powder X-ray diffraction (XRD), <sup>29</sup>Si MAS NMR, and chemical analyses. Perdeuterated alkane, *n*-hexane-*d*<sub>14</sub> (with 98% <sup>2</sup>H isotopic enrichment, purchased from Cambridge Isotope Laboratories, Inc.) was used without further purification.

**Sample Preparation.** To prepare samples for the NMR experiments, ~0.3 g of silicalite was loaded in a 5 mm (outer diameter) glass tube that was connected to a vacuum system. The sample was then heated at 720 K for 1.5 h in air and for 4 h under vacuum to a final pressure of 10<sup>-5</sup> Torr (1 Torr = 133.3 Pa) above the sample. After the sample was cooled back to room temperature, the silicalite was exposed to the vapor of previously degassed *n*-hexane-*d*<sub>14</sub> (ca. 8 Torr) in a calibrated volume (140 mL). A few minutes were required for the complete consumption of *n*-hexane vapor to occur. The adsorption procedure was repeated several times until the amount of adsorbed alkane was 915 μmol/g (5.5 molecules per unit cell). This step-by-step procedure for the alkane adsorption (60 μmol of *n*-hexane in each step) was used to avoid potentially possible condensation of the alkane on the outer surface of the silicalite crystallites. After adsorption, the neck of the tube was sealed off while the sample was maintained in liquid nitrogen, to prevent its heating by the flame. The sealed sample was then transferred into an NMR probe, so that the <sup>2</sup>H NMR spectra could be recorded.

**NMR Measurements.** <sup>2</sup>H NMR experiments were performed at 61.42 MHz on a Bruker model MSL-400 spectrometer, using a high-power probe with 5-mm horizontal solenoid coil. All <sup>2</sup>H NMR spectra were obtained by Fourier transformation of the quadrature-detected quadrupole echo, arising in a pulse sequence<sup>36</sup>

$$\left(\frac{\pi}{2}\right)_{\pm X} - \tau_1 - \left(\frac{\pi}{2}\right)_Y - \tau_2 - \text{acquisition} - t \quad (\text{i})$$

where  $\tau_1 = 30 \mu\text{s}$ ,  $\tau_2 = 34 \mu\text{s}$ ,  $t$  is a repetition time for sequence (i) during the accumulation of NMR signal. The duration of the  $\pi/2$  pulses was 4.0–5.0 μs. Spectra were typically obtained with 500–5000 scans and a repetition time of  $t = 0.4$ –2 s. Inversion–recovery experiments, to derive spin–lattice relaxation times ( $T_1$ ), were conducted using the pulse sequence<sup>37</sup>

$$(\pi)_X - t_v - \left(\frac{\pi}{2}\right)_{\pm X} - \tau_1 - \left(\frac{\pi}{2}\right)_Y - \tau_2 - \text{acquisition} - t \quad (\text{ii})$$

where  $t_v$  is a variable delay between the 180° ( $\pi$ )<sub>X</sub> inverting pulse (as in the standard inversion–recovery pulse sequence<sup>37</sup>) and quadrupole echo sequence (i). In the case of the overlapping of different signals to the overall <sup>2</sup>H NMR line shape,  $T_1$  values were calculated on the basis of the time  $\tau_0$  ( $\tau_0 = 0.693T_1$ ).  $\tau_0$  is the time for which the intensity of the NMR line changes from the inverted negative position to the normal positive one in the inversion–recovery experiment (sequence (ii)).

The temperature of the samples was controlled with a flow of nitrogen gas and stabilized with a variable-temperature unit (Bruker model BVT-1000) with a precision of ~1 K; the sample was allowed to equilibrate for at least 15 min at a given temperature before the NMR signal was acquired.

<sup>2</sup>H NMR line shapes were fitted to the theoretical powder patterns, using a nonlinear least-squares tensor-fitting routine.

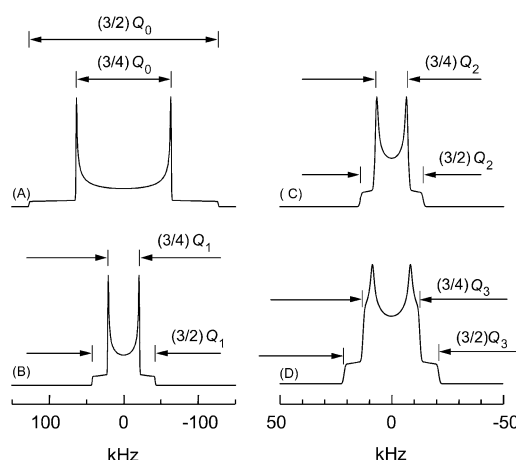


**Figure 1.** Theoretical <sup>2</sup>H NMR spectra of (A) a polycrystalline sample (static CD<sub>3</sub> group,  $C_Q^0 = e^2qQ/h = Q_0 = 169.5 \text{ kHz}$ ,  $\eta = 0$ ), (B) a rapid rotation of the CD<sub>3</sub> group about one C<sub>3</sub> axis (angle  $\alpha = 109.47^\circ$ ,  $Q_1 = (1/3)Q_0$ ), (C) a rapid rotation of the CD<sub>3</sub> group about two axes (angles  $\alpha = 109.47^\circ$  and  $\beta = 109.47^\circ$ ,  $Q_2 = (1/9)Q_0$ ), and (D) rapid hops with an angle  $\Theta = 86^\circ$  between two equally populated sites for a CD<sub>3</sub> group, rapidly rotating about the C<sub>3</sub> axis ( $Q_3 = (1/6)Q_0$ ,  $\eta = 0.2$ ). An individual line shape function of the form  $g(x) = [1/(\sigma\sqrt{2\pi})] \exp[-(x^2/(2\sigma^2))]$ , with  $\sigma = 0.5 \text{ kHz}$ , was used in all simulations.

**Theoretical Background.** <sup>2</sup>H NMR spectra from polycrystalline organic solids are known to be dominated by quadrupole coupling.<sup>32–34,38,39</sup> This coupling is of intramolecular origin<sup>32–34</sup> and is strongly affected by the mode and rate of the molecular motion in which a molecule is involved.<sup>33,39,40</sup>

For molecules that are rigid on the <sup>2</sup>H NMR time scale  $\tau_{\text{NMR}}$  (i.e., when the correlation times  $\tau_C$  for molecular reorientation and internal motions satisfy the condition  $\tau_C \gg \tau_{\text{NMR}} \approx Q_0^{-1} \approx 5 \times 10^{-6} \text{ s}$ , where  $Q_0 = C_Q^0 = e^2qQ/h$  is the quadrupole coupling constant, which is unaffected by any of motional averaging),<sup>41</sup> <sup>2</sup>H NMR spectra represent Pake-type powder patterns.<sup>32,33</sup> The dominant features of these line shapes are two strong peaks separated by the splitting  $(3/4)Q_0$  and two shoulders separated by  $(3/2)Q_0$  (see Figure 1A). For deuterium bonded to tetrahedral carbon atoms in polycrystalline organic solids,  $(3/4)Q_0$  is usually 120–130 kHz and the asymmetry parameter  $\eta$  is close to zero.<sup>38,40,42–44</sup> If a CD<sub>3</sub> group of an organic molecule undergoes fast 3-fold jumps or diffusional rotation about the C–CD<sub>3</sub> bond with a correlation time  $\tau_R \ll \tau_{\text{NMR}}$  (i.e.,  $\tau_R < 10^{-7}$ – $10^{-6} \text{ s}$  and if isotropic reorientation of the molecule as a whole is slow ( $\tau_C \gg \tau_{\text{NMR}}$ )), then the line shape of the spectrum for CD<sub>3</sub> groups will be similar to that of rigid molecules, but with the quadrupole splitting reduced to the value of  $(3/4)Q_1$  (Figure 1B),<sup>40,43,44</sup> according to the relation

$$Q_1 = Q_0 \left( \frac{3 \cos^2 \alpha - 1}{2} \right) \quad (1)$$

Here,  $\alpha$  is the rotation angle between the C–D and C–CD<sub>3</sub> bonds. For the ideal tetrahedral geometry of the C–CD<sub>3</sub> fragment,  $\alpha = 109.47^\circ$  and  $Q_1 = (1/3)Q_0$ . In practice, typical values of the reduced splitting  $(3/4)Q_0$  are 35–40 kHz.<sup>40,44</sup>

If a CD<sub>3</sub> group is involved in additional rotation (either 3-fold or higher-fold jumps) about a second axis tilted at an angle  $\beta$ , with respect to the first axis, then, again, its <sup>2</sup>H NMR spectrum has a quadrupole splitting reduced to  $(3/4)Q_2$ <sup>45</sup> (Figure 1C). If  $\beta$  is equal to  $\alpha$  ( $\alpha = 109.47^\circ$ ), then  $Q_2 = (1/9)Q_0$  and the splitting is typically  $(3/4)Q_2 \approx 12$ –14 kHz. Similarly, in the case of the existence of a third rotation (jump) axis with  $\alpha =$

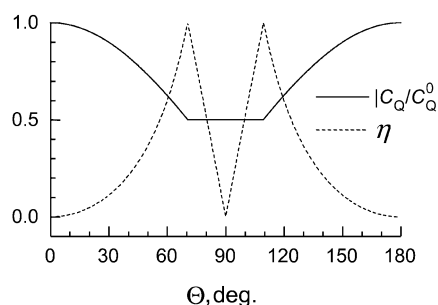


**Figure 2.** Predicted dependence of the effective values for  $\eta$  and  $C_Q$  vs  $\Theta$ , the angle between the directions of the principal axis of the quadrupole tensor ( $\eta = 0$ ), in the case of a rapid exchange between two equally populated sites.

109.47°, there will be a further reduction of the quadrupole splitting up to  $Q_3 = (1/27)Q_0$ .

Fast librations of the C–C bonds result in the decrease of the quadrupole splitting  $(3/4)Q_1$  of the rapidly rotating  $CD_3$  group. This decrease can be taken into account by the order parameter  $S$ , so that  $(3/4)Q_{1L} = (3/4)Q_1S$ , which is dependent on the deviation of the rotation axis from its mean position. Evaluation of the order parameter  $S$  requires detailed knowledge of the librational angle distribution function,<sup>46</sup> which usually is not available. To get an estimation of the magnitude of the librational angles, the model of “free diffusion in a cone” can be applied. Within the frame of this model the order parameter  $S_{\text{cone}}$  can be expressed as<sup>47,48</sup>

$$S_{\text{cone}} = \frac{\cos \gamma_0 (1 + \cos \gamma_0)}{2} \quad (2)$$

where  $\gamma_0$  ( $0^\circ \leq \gamma \leq \gamma_0$ ) is the cone semiangle.

If a  $CD_3$  group rapidly rotating around a C– $CD_3$  bond also exhibits fast exchange jumps between two sites, with an angle  $\Theta$  between the directions of the C–C bonds in each position, the quadrupole splitting is reduced further and anisotropy appears in the spectrum (Figure 1D). The dependence of  $\eta$  and the quadrupole constant  $C_Q$  versus the angle  $\Theta$  is defined in the following manner:

$$\frac{C_Q}{C_Q^0} = \frac{1}{2} \text{ and } \eta = 3|\cos \Theta| \quad \left( \text{at } |\cos \Theta| \leq \frac{1}{3} \right)$$

$$\frac{C_Q}{C_Q^0} = \frac{1}{4}(1 + 3|\cos \Theta|) \text{ and } \eta = 3\left(\frac{1 - |\cos \Theta|}{1 + 3|\cos \Theta|}\right)$$

$$\left( \text{at } \frac{1}{3} \leq |\cos \Theta| \leq 1 \right) \quad (3)$$

Here,  $C_Q$  is an effective value of the quadrupole constant in the presence of exchange, and  $C_Q^0$  is the quadrupole constant in the absence of exchange. The predicted dependence of effective values for  $\eta$  and  $C_Q$  versus the angle  $\Theta$  between directions of the axial axis of the quadrupole tensor ( $\eta = 0$  in the absence of exchange), in the case of rapid exchange between two equally populated sites, is also given in Figure 2.

When the correlation time  $\tau_C$  for the isotropic reorientation (rotation) of the molecule as a whole becomes comparable to  $\tau_{\text{NMR}}$ , a broadening of the spectrum is observed and the sharp features disappear.<sup>41</sup> For rapid isotropic reorientation, as in liquids, when  $\tau_C \ll \tau_{\text{NMR}}$ , the quadrupole splitting is averaged to zero and a single line with a Lorentzian shape is observed at  $\omega_1$ , which is the Larmor frequency of the deuterium nucleus.<sup>34</sup>

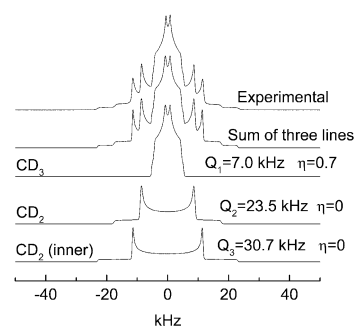


**Figure 3.**  $^2\text{H}$  NMR spectrum at 303 K for *n*-hexane- $d_{14}$  adsorbed on silicalite and its decomposition in three Pake-powder patterns from the  $CD_3$  and  $CD_2$  groups with  $C_Q$  and  $\eta$  parameters, indicated above each separate simulated spectrum.

Although the  $^2\text{H}$  NMR line shape provides information about the type of motion for a  $CD_3$  group in a molecule, it contains no further information about the rates of this process. For many experimental situations, this information may be obtained from the special measurements of nuclear relaxation rates,  $1/T_1$ . For anisotropically reorienting methyl group in a static solid (3-fold jumps or continuous diffusion of a  $CD_3$  group about a  $C_3$  symmetry axis), explicit expressions for  $T_1$  were developed by Torchia and Szabo.<sup>49</sup> For example, for the 3-fold jump model of the methyl group reorientation, the following expression for  $T_1$  is valid:<sup>49</sup>

$$\frac{1}{T_1} = \frac{1}{8} \left( \frac{3}{2} \pi C_Q \right)^2 \left\{ \frac{\tau_R}{1 + \omega_1^2 \tau_R^2} \left[ \sin^2 2\alpha (\cos^2 \theta + \cos^2 2\theta) + \sin^4 \alpha \left( \sin^2 \theta + \frac{1}{4} \sin^2 2\theta \right) - 8 \sin^3 \alpha \cos \alpha \right. \right.$$

$$\left. \left. (\sin^3 \theta \cos \theta) \cos 3\Phi \right] + \frac{\tau_R}{1 + 4\omega_1^2 \tau_R^2} \left[ 4 \sin^2 2\alpha (\sin^2 \theta + \frac{1}{4} \sin^2 2\theta) + \sin^4 \alpha (1 + 6 \cos^2 \theta + \cos^4 \theta) + 8 \sin^3 \alpha \cos \alpha (\sin^3 \theta \cos \theta) \cos 3\Phi \right] \right\} \quad (4)$$

where  $\tau_R$  is the correlation time of the 3-fold rotational jumps,  $\theta$  and  $\Phi$  are the polar angles describing the orientation of the rotation axis for the  $CD_3$  group, with respect to the external magnetic field  $B_0$ , and  $\alpha$  is the angle between the rotation axis and the principal axis of the axial electric-field-gradient tensor (the direction of the C–D bond).  $\theta = 90^\circ$  at the perpendicular edges of the powder pattern, whereas  $\alpha \approx 109.47^\circ$  for the methyl group.

## Results and Discussion

**Analysis of the  $^2\text{H}$  NMR Line Shape for the Adsorbed *n*-Hexane.** Figure 3 shows the  $^2\text{H}$  NMR spectrum for *n*-hexane- $d_{14}$  adsorbed on silicalite for a loading of 5.5 molecules per unit cell. The spectrum retains its total line shape, which is unchanged within the 143–413 K temperature range. A computer decomposition and parameter fitting of the total spectrum indicates that it represents a superposition of the three distinct powder patterns with three couples of spectral parameters (quadrupole constants  $C_Q$  and asymmetry parameters  $\eta$ ; see Table 1). It should be noted that the spectrum retains the same line shape for loadings of two and four molecules per unit cell.

The values of  $C_Q^0$  usually fall in the range of 160–190 kHz for rigid aliphatic deuterons<sup>38,40,42–44</sup> and  $C_Q^0 = 168$  kHz for



**TABLE 1: Characteristics of the Powder Patterns of the  $^2\text{H}$  NMR Spectra**

	$C_Q$ , <sup>a</sup> kHz	$\eta$ <sup>a</sup>	$\Theta$ , <sup>b</sup> deg	$C_Q^0$ , <sup>c</sup> kHz	$S^d$
CD <sub>3</sub>	7.0	0.7	103.5 or 116.8	14	0.500
CD <sub>2</sub>	23.5	0	0 or 90	47	0.560
CD <sub>2</sub> (inner)	30.7	0	0 or 90	61.4	0.731

<sup>a</sup> Values were of the CD<sub>n</sub> groups of *n*-hexane-*d*<sub>14</sub> adsorbed on silicalite. <sup>b</sup> Possible values of the angle  $\Theta$  between the end-to-end vector of the molecule before and after the jump in two adjacent adsorption sites. <sup>c</sup> Averaged by local movements at the adsorption site. <sup>d</sup> Order parameter for the CD<sub>n</sub> groups of the alkane locally moving inside the zeolite channel.

the CD<sub>2</sub> groups of *n*-hexane-*d*<sub>14</sub>.<sup>50</sup> Reduced values of the experimentally observed  $C_Q$  values, compared to the  $C_Q^0$  value in rigid adsorbed *n*-hexane-*d*<sub>14</sub>,<sup>50</sup> and the appearance of asymmetry in the powder pattern of the methyl groups indicate that adsorbed *n*-hexane is involved in some fast anisotropic motion. The expected fast rotation of the terminal CD<sub>3</sub> group around the C<sub>1</sub>–C<sub>2</sub> (C<sub>5</sub>–C<sub>6</sub>) bond implies a reduction of its quadrupole constant by a factor of 3, in comparison to that of nonterminal CD<sub>2</sub> groups. Therefore, the signals with  $C_Q = 23.5$  and 30.7 kHz are assigned to the CD<sub>2</sub> groups and the signal with the smaller quadrupole constant,  $C_Q = 7.0$  kHz, is assigned to the methyl CD<sub>3</sub> groups.

One can envisage three types of translational motion for *n*-hexane that are captured by the three-dimensional system of interconnecting channels of silicalite,<sup>5</sup> namely, along the straight channels, along the zigzag channels, and along a tortuous path between the straight and zigzag channels via the intersection region. In the following discussion, we interpret the observed  $^2\text{H}$  NMR line shapes in relation to these possible modes of *n*-hexane motion.

Theoretical MD<sup>16</sup> and Monte Carlo<sup>17,51</sup> simulations, as well as experimental QENS<sup>9</sup> results, predict equal probabilities of *n*-hexane molecules being located inside both zigzag and straight channels and a very fast (hundreds of picoseconds) exchange for the *n*-hexane molecules between the two types of channels in the process of translational diffusion. Therefore, it is reasonable to assume that the observed line shapes reflect the averaging of the  $^2\text{H}$  quadrupole tensor due to jumps between segments of the straight channels, segments of the zigzag channels, or an interchange between the zigzag and straight channels.

Local averaging arising from the possible rotation of the molecule as a whole around the channel axis and trans/gauche conformational isomerization (internal rotation of the CD<sub>2</sub> groups) in the narrow channels,  $\sim 5.5$  Å in diameter, should lead to a quadrupole tensor that is approximately axial (see, e.g., the example of alkane/urea inclusion compounds in the work of Cannarozzi et al.<sup>52</sup> and El Baghdadi et al.<sup>53</sup>). Therefore, it is reasonable to assume that a notable value of the asymmetry parameter for the methyl group ( $\eta = 0.7$ ) originates from an uniaxial averaging of the quadrupole tensor in the process of jumps among energetically equivalent adsorption sites inside straight and zigzag channels.<sup>16,17</sup> For a simple model of jumps between two adjacent adsorption sites, we can estimate both the angle  $\Theta$  (which is the angle between the end-to-end vector of the molecule before and after the jump) and the value of  $C_Q^0$  averaged only by local movements at a given adsorption site (see Figure 2). Two possible values of  $\Theta$  could be found (Table 1) for CD<sub>3</sub>, using the predicted dependence of the effective values  $\eta$  and  $C_Q$  vs  $\Theta$  (Figure 2). Both values of  $\Theta_1$  ( $\sim 103.5^\circ$  and  $116.8^\circ$ ) are in the vicinity of the angles between the straight and zigzag channels ( $\Theta = 90^\circ$ ) or between segments of zigzag

channels ( $\Theta \approx 112.6^\circ$ ) of the zeolite framework. Therefore, the observed value of  $\eta$  for CD<sub>3</sub> can reflect the interchange of the alkane molecules between both the straight and zigzag channels or between neighboring segments of the zigzag channels.

Zero values of the asymmetry parameter  $\eta$  for the CD<sub>2</sub> groups may correspond to the exchange between either neighboring segments of the straight channels ( $\Theta = 0^\circ$ ) or between zigzag and straight channels ( $\Theta = 90^\circ$ ) (see Figure 2). The translational movement of the molecule exclusively along the straight channels should not result to a reduction of the value of  $C_Q$  to 23.7 or 30.7 kHz. Only a factor-of-2 reduction of the value of  $C_Q^0$  is expected, because of the rotation of the molecule around the channel axis (vide infra). A larger reduction of the  $C_Q^0$  value indicates that  $C_Q$  results from the exchange between segments of zigzag channels or between straight and zigzag channels with the effective value of  $\Theta = 90^\circ$ .

Therefore, the experimentally observed  $\eta$  and  $C_Q$  values could not be assigned unequivocally to the exchange between certain types of channels. We can conclude that  $\eta$  and  $C_Q$  correspond to the fast exchange of the molecules among both types of channels with some effective angle  $\Theta \approx 90^\circ$  between neighboring adsorption sites.

The value of  $C_Q^0$  averaged only by local movements at a given adsorption site inside the channel, i.e., without averaging by jumps between adjacent adsorption sites, can be further calculated (eq 3) on the basis of the estimated values of  $\Theta$  (Table 1). These values of  $C_Q^0$  reflect the local motion of the CD<sub>n</sub> groups for the alkane located inside the zeolite channel.

Long-chain alkanes located in one-dimensional channels 5.5 Å in diameter (urea/inclusion compounds) are known to undergo uniaxial rotational diffusion about the main molecular axis, parallel to the channel axis.<sup>52,53</sup> It was also found by QENS<sup>9</sup> that *n*-hexane that is located inside a channel of ZSM-5 zeolite rotates rapidly about the channel axis. This uniaxial rotation with the angle  $\alpha = 90^\circ$  between a C–D bond and the main molecular axis, which is parallel to the direction of the channel axis, should result in a reduction of the observed value of  $C_Q$  by a factor of 2, with respect to  $C_Q^0$  in the rigid alkane (eq 1). The value of  $C_Q$  of the methyl group also rotating around the terminal CD<sub>3</sub>–CD<sub>2</sub> bond is reduced additionally by a factor of 3.

A further reduction of the quadrupole constants can be explained in terms of librational motion of the CD<sub>3</sub> and CD<sub>2</sub> groups<sup>54–57</sup> or by invoking the presence of gauche conformations<sup>58</sup> in the hydrocarbon chain. For the model of librational motion in a cone, the experimentally observed order parameters (Table 1)  $S_1(\text{CD}_3) = 0.500$ ,  $S_2(\text{CD}_2) = 0.560$ , and  $S_3(\text{CD}_2) = 0.731$  should correspond to the librational angles  $\gamma_0 = 52^\circ$  (CD<sub>3</sub>),  $\gamma_0 = 48^\circ$  (CD<sub>2</sub>), and  $\gamma_0 = 36^\circ$  (CD<sub>2</sub>). However, for a linear *n*-hexane molecule with a diameter perpendicular to the main (long) molecular axis of 4.5 Å,<sup>15</sup> the maximum value of  $\gamma_0$  could be  $\sim 6^\circ$  in the narrow zeolite channels that have a diameter of 5.5 Å. Moreover, similar values of  $\gamma_0$  would be expected for the different CD<sub>3</sub> and CD<sub>2</sub> groups in the molecule, when librated as a whole.<sup>57</sup> Therefore, the reduced quadrupole constants and three different order parameters  $S_1$ ,  $S_2$ ,  $S_3$  cannot be accounted for by a librational motion of the molecule as a whole.

The other possibility for a further reduction of the quadrupole constants is the trans/gauche conformational isomerization in the adsorbed alkane.<sup>58</sup> If the molecule inside a channel is in the “all-trans” state, the molecule is perfectly linear, and only uniaxial rotation of the molecule about its long molecular axis

**TABLE 2: Definition of Probabilities  $P_i$  of Finding a *n*-Hexane Molecule in Silicalite in the Conformational State  $i$** 

Order Parameters	
$S_1$	0.500
$S_2$	0.560
$S_3$	0.731
Conformers $i^a$	
	$P_i$
	$P'_t = 0.783 \pm 0.05, P_t = 0.735 \pm 0.04$
tt	$P'_t P_t = 0.576 \pm 0.068$
tg	$P'_t(1 - P_t) = 0.207 \pm 0.044$
gt	$(1 - P'_t)P_t = 0.159 \pm 0.042$
gg	$(1 - P'_t)(1 - P_t) = 0.058 \pm 0.022$

<sup>a</sup> Here, tt denotes an *n*-alkane chain with both C<sub>3</sub>–C<sub>4</sub> and C<sub>2</sub>–C<sub>3</sub> bonds in the “trans” conformation, tg denotes an *n*-alkane chain with a gauche bond at the position of the C<sub>2</sub>–C<sub>3</sub> bond, and gt denotes an *n*-alkane chain with a gauche bond at the position of the C<sub>3</sub>–C<sub>4</sub> bond.

can be responsible for the reduction of the quadrupole constant. The observed  $C_Q$  values would be 84 and 28 kHz for CD<sub>2</sub> and CD<sub>3</sub> groups, respectively. Fast conformational interchange of the hydrocarbon chain of *n*-hexane between gauche/trans (gt), trans/trans (tt), and trans/gauche (tg) conformations can be responsible for the further reduction of the quadrupole constants, which is similar to the case of long-chain alkanes that are located in one-dimensional channels formed by the hydrogen-bonded network of urea molecules (alkane/urea inclusion compounds).<sup>52,53</sup>

If gauche conformations occur about both the C<sub>2</sub>–C<sub>3</sub> and C<sub>3</sub>–C<sub>4</sub> bonds of *n*-hexane, three reduced quadrupole constants should be observed,<sup>52,53</sup> as is the case experimentally. The order parameters are related to the probabilities of trans populations associated with the C<sub>2</sub>–C<sub>3</sub> or C<sub>3</sub>–C<sub>4</sub> bonds in the following manner:<sup>48,52</sup>

$$S_1(\text{CD}_3) = P_t - P'_t + P'_t P'_t \quad (5)$$

$$S_2(\text{CD}_2) = \frac{1}{2}(P_t + P'_t + P'_t P'_t - 1) \quad (6)$$

$$S_3(\text{CD}_2)_{\text{inner}} = P'_t \quad (7)$$

Here,  $S_1 = 6C_Q^{(\text{CD}_3)}/C_Q^0$ ,  $S_2 = 2C_Q^{(\text{CD}_2)}/C_Q^0$ , and  $S_3 = 2C_Q^{(\text{CD}_2)_{\text{inner}}}/C_Q^0$ .  $P'_t$  is the trans population associated with the C<sub>3</sub>–C<sub>4</sub> bond, or it is the probability of having a tg defect (gauche conformation at the C<sub>2</sub>–C<sub>3</sub> bond);  $P_t$  is the trans population associated with the C<sub>2</sub>–C<sub>3</sub> bond, or it is the probability of having a gt defect (gauche conformation at the C<sub>3</sub>–C<sub>4</sub> bond). From the calculated probabilities  $P'_t$  and  $P_t$  on the basis of the order parameters  $S$ , one can further derive the probabilities  $P_i$  for each of the conformers (see Table 2).

It follows from Table 2 that the proportion percentage of trans/gauche conformers for the central C<sub>3</sub>–C<sub>4</sub> bond of the *n*-alkane, 78/22, can be responsible for the reduction of the quadrupole constants. The estimated percentage of tg conformers is less than the percentage calculated theoretically for molecules that are located in the straight channels by MD simulations (86/14).<sup>16</sup> However, it is higher than that for liquid *n*-hexane (70/30)<sup>16,59</sup> or in the gas phase (50/50).<sup>15</sup> It follows from the reduction of the quadrupole constant for the adsorbed *n*-alkane that the constraining effect of the narrow zeolite pore walls forces the sorbate *n*-alkane molecule into a more elongated shape, compared to that of the molecule in the liquid or ideal gas states. Thus, the presence of gauche defects at either C<sub>2</sub>–C<sub>3</sub> or C<sub>3</sub>–C<sub>4</sub> bonds provides a further reduction of the quadrupole constants.

Finally, the observed <sup>2</sup>H NMR line shape for *n*-hexane adsorbed in silicalite can be interpreted in terms of motional

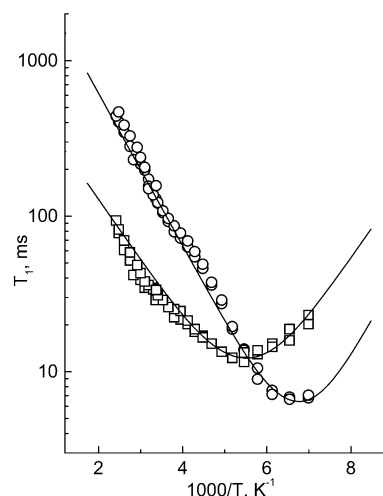


**Figure 4.** Temperature dependence of <sup>2</sup>H NMR spin–lattice relaxation times ( $T_1$ ) measured at perpendicular edges of powder patterns for (□) CD<sub>2</sub> and (○) CD<sub>3</sub> groups for *n*-hexane-*d*<sub>14</sub> adsorbed on silicalite. The best fits (solid lines) to  $T_1$  were obtained on the basis of theoretical expression (4) with  $\alpha = 109.47^\circ$ , the dynamic characteristics given in Table 3, and effective  $C_Q(\text{CD}_3)$  and  $C_Q(\text{CD}_2)$  values of 116 and 160 kHz, respectively. The contribution to the spin–lattice relaxation times at the perpendicular edges of the powder pattern is the weighted average of  $T_1$  from the two contributing orientations with  $\theta = 90^\circ$  and  $35.3^\circ$ .<sup>49</sup> The relative weights of these orientations are 0.625 and 0.375, respectively. The value of  $\Phi$  was averaged over all possible orientations.

**TABLE 3: Dynamic Characteristics for the Reorientation of CD<sub>3</sub> and CD<sub>2</sub> Groups for *n*-Hexane Adsorbed in Silicalite**

	CD <sub>3</sub> groups	CD <sub>2</sub> groups
pre-exponential factors, $\tau_0$ (ps)	1.0	14.5
energy barrier, $E_a$ (kJ/mol)	9.4	7.5

behavior that is exhibited by both internal CD<sub>*n*</sub> groups and the molecule as a whole. The motion can be represented as (i) a rotation of the molecule as a whole around the channel axis; (ii) fast jumps of the molecule by some effective angle 90° among the neighboring adsorption sites in the straight and zigzag channels; (iii) fast tg interconversions for the molecule inside the channels, with the probability of finding the molecule in tg states being 78/22; and (iv) fast rotation of the terminal methyl groups around the C–C bonds.

**Analysis of Spin–Lattice Relaxation Time.** The spin–lattice relaxation time  $T_1$  for both CD<sub>3</sub> and CD<sub>2</sub> of the adsorbed *n*-hexane-*d*<sub>14</sub> was measured as a function of temperature in the range of 143–383 K (Figure 4). The logarithm of  $T_1$  versus the reciprocal temperature ( $1/T$ ) exhibits minima for CD<sub>3</sub> and CD<sub>2</sub> groups, where  $\omega_1\tau_C \approx 1$ , at different temperatures (153 and 183 K, respectively). This indicates that reorientational correlation times are different for CD<sub>3</sub> and CD<sub>2</sub>, and different modes of molecular motion can explain the  $T_1$  relaxation. It is reasonable to suggest that the fast rotation around the CD<sub>3</sub>–CD<sub>2</sub> bond is responsible for the relaxation of the methyl groups, whereas tg isomerization (internal rotation of the CD<sub>2</sub> groups) is responsible for the relaxation of the CD<sub>2</sub> groups. Therefore, the experimental  $T_1$  data were fitted with expression (4) of Torchia and Szabo<sup>49</sup> as a rough approximation to derive the dynamics characteristics for the adsorbed *n*-hexane. It was also assumed that reorientational correlation times  $\tau_R$  have an Arrhenius-type temperature behavior, i.e.,  $\tau_R = \tau_{R0} \exp[E_R/(RT)]$  for both CD<sub>3</sub> and CD<sub>2</sub>. The best fits to the temperature dependencies of  $T_1$  were obtained with the dynamic characteristics that are presented in Table 3.

The derived values of  $E_R$  for CD<sub>3</sub> and CD<sub>2</sub> groups are in good agreement with the energy barriers for torsional rotation

of the terminal methyl groups or tg conformational isomerization around nonterminal C—C bonds in alkanes.<sup>11,60,61</sup> Correlation times of  $\tau_R \approx 40$ –300 ps at 300 K for these motions are also in good agreement with the characteristic times for torsional motion in alkanes.<sup>11,16,30,61</sup>

From the analysis of the line shape of the adsorbed alkane (vide supra), we have concluded that three modes of molecular motion affect the  $^2\text{H}$  NMR line shape: conformational isomerization (for a methyl group, it is a rotation around the terminal C—C bond), uniaxial rotation of the molecule inside the zeolite channels, and exchange of the molecule between straight and zigzag channels, the latter of which corresponds to the translational diffusion along the zeolite framework. According to the estimated values for  $E_R$  and  $\tau_R$ , only a rotation of the methyl groups around the terminal C—C bonds is responsible for the relaxation of the methyl groups. At the same time, the values of  $E_R$  and  $\tau_R$  for the  $\text{CD}_2$  groups cannot be assigned to some certain mode of motion unambiguously. The estimated value of  $\tau_R \approx 300$  ps can correspond to both conformational isomerization and translational diffusion. Indeed, the rates of interchange of the alkane molecules between the straight and zigzag channels and conformational isomerization are similar and are of the order of 100 ps, as predicted from MD simulations.<sup>16</sup> QENS data also give a value on the order of 100 ps for the molecule residence time inside a channel during the process of translational diffusion.<sup>9</sup> Moreover, the estimated value of  $E_R = 7.5$  kJ/mol is less than any ever estimated for tg interconversions (9–13 kJ/mol) and may be considered to be close to  $E_R = 5$  kJ/mol, as derived for translational diffusion from QENS data.<sup>9</sup> Therefore, one can expect that these modes of motion, translational diffusion and conformational isomerization, could provide similar contributions to  $T_1$ .

## Conclusion

The analysis of the  $^2\text{H}$  NMR line shape and the spin-lattice relaxation times for perdeuterated *n*-hexane adsorbed in silicalite allowed us to characterize the peculiarities of the motional behavior of the adsorbed alkane. The observed line shape and the spin-lattice relaxation time are affected by both fast translational and rotational motions. The translational motion of the adsorbed *n*-hexane consists of fast interchanges between segments of straight channels or between straight and zigzag channels with an effective angle of  $\Theta \approx 90^\circ$  between adjacent sites of the molecule location in successive jumps. The molecule, which is located inside the zeolite channels, is involved in two modes of rotational motion, uniaxial rotation about the channel axis and internal rotations: gauche/trans conformational isomerization around nonterminal  $\text{CD}_2$ — $\text{CD}_2$  bonds and rotation of the methyl groups around terminal  $\text{CD}_3$ — $\text{CD}_2$  bonds. The narrow zeolite pore walls constrain the molecules in a more elongated shape than that in the ideal gas or liquid states, and the proportional percentage of trans/gauche conformers for the central C—C bond of the *n*-alkane was estimated to be 78/22. The rotation of the methyl groups occurs with a characteristic time of  $\sim 40$  ps at 300 K and an activation energy of 9.4 kJ/mol. The reorientation of the methylene groups, which corresponds either to conformational isomerization or to translational diffusion, occurs 1 order of magnitude slower, with a characteristic time of  $\sim 300$  ps and an activation energy of 7.5 kJ/mol.

**Acknowledgment.** The authors wish to express their gratitude to M. M. Alkaev for the simulation of the  $^2\text{H}$  NMR spectra and to Dr. A. Tuel for providing the silicalite sample. This

research was made possible, in part, with financial support from INTAS (Grant No. 96-1177) and RFBR (Grant No. 00-03-22002).

## References and Notes

- (1) Yang, R. T. *Gas Separation in Adsorption Processes*; Butterworth Publishers: Stoneham, MA, 1987.
- (2) Karger, J.; Ruthven, D. M. *Diffusion in Zeolites and Other Microporous Solids*; Wiley-Interscience: New York, 1992.
- (3) Chang, C. D. *Catal. Rev. Sci. Eng.* **1983**, 25, 1.
- (4) Kokotailo, G. T.; Lawton, S. L.; Olson, D. H.; Meier, W. M. *Nature (London)* **1978**, 272, 437. Olson, D. H.; Kokotailo, G. T.; Lawton, S. L.; Meier, W. M. *J. Phys. Chem.* **1981**, 85, 2238.
- (5) Flanigen, E. M.; Bennet, J. M.; Grosse, R. W.; Cohen, J. P.; Patton, R. L.; Kirchner, R. M.; Smith, J. V. *Nature (London)* **1978**, 271, 512.
- (6) Krishna, R.; Smit, B.; Vlugt, T. J. H. *J. Phys. Chem. A* **1998**, 102, 7727.
- (7) Dwyer, J. *Nature (London)* **1989**, 339, 174. Chen, N. Y.; Kaeding, W. W.; Dwyer, J. *J. Am. Chem. Soc.* **1979**, 101, 6783. Chen, N. Y.; Degnan, J. T. F.; Smith, C. M. *Molecular Transport and Reactions in Zeolites. Design and Application of Shape Selective Catalysts*; VCH Publishers: Weinheim, Germany, 1994.
- (8) Heink, W.; Karger, J.; Naylor, T.; Winkler, U. *Chem. Commun.* **1999**, 57. Karger, J.; Bar, N. K.; Heink, W.; Pfeifer, H.; Seiffert, G. Z. *Naturforsch. A* **1995**, 50, 186. Heink, W.; Karger, J.; Pfeifer, H.; Stallmach, F. *J. Am. Chem. Soc.* **1990**, 112, 2175.
- (9) Jobic, H.; Bee, M.; Caro, J. *Proceedings of the 9th International Zeolite Conference*, Montreal, 1992; von Ballmoos, R., Higgins, J. B., Treacy, M. M. J., Eds.; Butterworth-Heinemann: Boston, MA, 1993; Vol. II, p 121.
- (10) Jobic, H.; Bee, M. *Z. Phys. Chem.* **1995**, 189, 179.
- (11) Stepanov, A. G.; Shubin, A. A.; Luzgin, M. V.; Jobic, H.; Tuel, A. *J. Phys. Chem. B* **1998**, 102, 10860.
- (12) Jobic, H. *Phys. Chem. Chem. Phys.* **1999**, 1, 525.
- (13) Millot, B.; Methivier, A.; Jobic, H.; Moueddeb, H.; Bee, M. *J. Phys. Chem. B* **1999**, 103, 1096.
- (14) Catlow, C. R. A.; Freeman, C. M.; Vessal, B.; Tomlinson, S. M.; Leslie, M. J. *Chem. Soc., Faraday Trans.* **1991**, 87, 1947.
- (15) June, R. L.; Bell, A. T.; Theodorou, D. N. *J. Phys. Chem.* **1990**, 94, 1508.
- (16) June, R. L.; Bell, A. T.; Theodorou, D. N. *J. Phys. Chem.* **1992**, 96, 1051.
- (17) Smit, B.; Siepmann, J. I. *J. Phys. Chem.* **1994**, 98, 8442.
- (18) Maginn, E. J.; Bell, A. T.; Theodorou, D. N. *J. Phys. Chem.* **1996**, 100, 7155.
- (19) Runnebaum, R. C.; Maginn, E. J. *J. Phys. Chem. B* **1997**, 101, 6394.
- (20) Webb, E. B., III; Grest, G. S. *Catal. Lett.* **1998**, 56, 95.
- (21) Webb, E. B., III; Grest, G. S.; Mondello, M. *J. Phys. Chem. B* **1999**, 103, 4949.
- (22) Bouyermaouen, A.; Bellemans, A. *J. Chem. Phys.* **1998**, 108, 2170.
- (23) Clark, L. A.; Ye, G. T.; Gupta, A.; Hall, L. L.; Snurr, R. Q. *J. Chem. Phys.* **1999**, 111, 1209.
- (24) Silbernagel, B. G.; Garcia, A. R.; Newsam, J. M.; Hulme, R. J. *Phys. Chem.* **1989**, 93, 6506.
- (25) Sato, T.; Kunimori, K.; Hayashi, S. *Phys. Chem. Chem. Phys.* **1999**, 1, 3839.
- (26) Boddenberg, B.; Burmeister, R. *Zeolites* **1988**, 8, 480. Boddenberg, B.; Burmeister, R. *Zeolites* **1988**, 8, 488. Burmeister, R.; Boddenberg, B.; Verfurden, M. *Zeolites* **1989**, 9, 318.
- (27) Eckman, R. R.; Vega, A. J. *J. Phys. Chem.* **1986**, 90, 4679.
- (28) Vega, A. J.; Luz, Z. *J. Phys. Chem.* **1987**, 91, 374.
- (29) Stepanov, A. G.; Maryasov, A. G.; Romannikov, V. N.; Zamaraev, K. I. *Magn. Reson. Chem.* **1994**, 32, 16.
- (30) Stepanov, A. G.; Alkaev, M. M.; Shubin, A. A. *J. Phys. Chem. B* **2000**, 104, 7677.
- (31) Kustanovich, I.; Fraenkel, D.; Luz, Z.; Vega, S.; Zimmermann, H. *J. Phys. Chem.* **1988**, 92, 4134. Kustanovich, I.; Vieth, H. M.; Luz, Z.; Vega, S. *J. Phys. Chem.* **1989**, 93, 7427.
- (32) Mehring, M. *Principles of High-Resolution NMR in Solids*. In *NMR Basic Principles and Progress*; Diehl, P., Fluck, E., Kosfeld, R., Eds.; Springer-Verlag: New York, 1976; Vol. 11.
- (33) Spiess, H. W. *Rotation of Molecules and Nuclear Spin Relaxation*. In *NMR Basic Principles and Progress*; Diehl, P., Fluck, E., Kosfeld, R., Eds.; Springer-Verlag: New York, 1978; Vol. 15, p 55.
- (34) Abragam, A. *The Principles of Nuclear Magnetism*; Oxford University Press: Oxford, U.K., 1961.
- (35) Tuel, A.; Ben Taarit, Y. *Microporous Mater.* **1994**, 2, 515.
- (36) Powles, J. G.; Strange, J. H. *Proc. Phys. Soc.* **1963**, 82, 6. Davis, J. H.; Jeffery, K. R.; Bloom, M.; Valic, M. I.; Higgs, T. P. *Chem. Phys. Lett.* **1976**, 42, 390.



- (37) Farrar, T. C.; Becker, E. D. *Pulse and Fourier Transform NMR. Introduction to Theory and Methods*; Academic Press: New York and London, 1971.
- (38) Smith, I. C. P. Deuterium NMR. In *NMR of Newly Accessible Nuclei*; Laszlo, P., Ed.; Academic Press: London, 1983; Vol. 2, p 1.
- (39) Jelinski, L. W. Deuterium NMR of Solid Polymers. In *High-Resolution NMR Spectroscopy of Synthetic Polymers in Bulk (Methods and Stereochemical Analysis)*; Komoroski, R. A., Ed.; VCH Publishers: New York, 1986; Vol. 7, p 335.
- (40) Barnes, R. G. *Adv. Nucl. Quadrupole Reson.* **1974**, *1*, 335.
- (41) Stocktone, G. W.; Polnaszek, C. F.; Tulloch, A. P.; Hasan, F.; Smith, I. C. P. *Biochemistry* **1976**, *15*, 954.
- (42) Mantsch, H. H.; Saito, H.; Smith, I. C. P. *Prog. Nucl. Magn. Reson. Spectrosc.* **1977**, *11*, 211.
- (43) Boddenberg, B.; Grosse, R. Z. *Naturforsch., A: Phys. Sci.* **1986**, *41*, 1361.
- (44) Rinne, M.; Depireux, J. *Adv. Nucl. Quadrupole Reson.* **1974**, *1*, 357.
- (45) Schwartz, L. J.; Meirovitch, E.; Ripmeester, J. A.; Freed, J. H. *J. Phys. Chem.* **1983**, *87*, 4453.
- (46) Fyfe, C. A.; Gobbl, G. C.; Hartman, J. S.; Klinowski, J.; Thomas, J. M. *J. Phys. Chem.* **1982**, *86*, 1247.
- (47) Petersen, N. O.; Chan, S. I. *Biochemistry* **1977**, *16*, 2657.
- (48) Wittebort, R. J.; Szabo, A. *J. Chem. Phys.* **1978**, *69*, 1722.
- (49) Torchia, D. A.; Szabo, A. *J. Magn. Reson.* **1982**, *49*, 107.
- (50) The quadrupole constant  $Q_0 = C_O^0$  for adsorbed *n*-hexane, which is not motionally reduced, was measured to be 168 kHz at 103 K.
- (51) Maginn, E. J.; Bell, A. T.; Theodorou, D. N. *J. Phys. Chem.* **1995**, *99*, 2057.
- (52) Cannarozzi, G. M.; Meresi, G. H.; Vold, R. L.; Vold, R. R. *J. Phys. Chem.* **1991**, *95*, 1525.
- (53) El Baghdadi, A.; Dufourc, E. J.; Guillaume, F. *J. Phys. Chem.* **1996**, *100*, 1746.
- (54) Gilson, D. F. R.; McDowell, C. A. *Mol. Phys.* **1961**, *4*, 125.
- (55) Casal, H. L.; Cameron, D. G.; Kelusky, E. *J. Chem. Phys.* **1984**, *80*, 1407.
- (56) Greenfield, M. S.; Vold, R. L.; Vold, R. R. *J. Chem. Phys.* **1985**, *83*, 1440.
- (57) Henry, E. R.; Sabo, A. *J. Chem. Phys.* **1985**, *82*, 4753.
- (58) Vold, R. L.; Vold, R. R.; Heaton, N. J. *Adv. Magn. Reson.* **1989**, *13*, 17.
- (59) Leggeter, S.; Tildesley, D. J. *Mol. Phys.* **1989**, *68*, 519.
- (60) Smith, J.; Karplus, M. *J. Am. Chem. Soc.* **1992**, *29*, 801.
- (61) Stepanov, A. G.; Alkaev, M. M.; Shubin, A. A.; Luzgin, M. V.; Shegai, T. O.; Jobic, H. *J. Phys. Chem. B* **2002**, *106*, 10114.